JOURNAL OF COMPUTATIONAL PHYSICS 16, 324–341 (1974)

A Cubic Spline Method for Solving the Wave Equation of Nonlinear Optics*

J. A. FLECK, JR.

University of California, Lawrence Livermore Laboratory, Livermore, California 94550

Received March 12, 1974; revised July 30, 1974

A numerical solution method is outlined for solving Maxwell's wave equation in parabolic approximation, which is of importance in nonlinear optics. The method is based on cubic splines which guarantee continuity of first and second derivatives. In practice the method has proven to be both accurate and flexible.

INTRODUCTION

Since the discovery of the laser a wide range of nonlinear optical effects has been observed experimentally and studied theoretically. One class of these effects results from the dependence of the refractive index of a medium on the intensity of the laser beam propagating through it. This dependence can result in either self-focusing [1–3] or self-defocusing [4, 5] of the beam, depending on whether the medium refractive index is an increasing or a decreasing function of beam intensity. The phenomenon of self-focusing has taken on great practical significance since the discovery that glass exhibits self-focusing at sufficiently low intensities to place significant limitations on the design of high power lasers utilizing neodymium in glass as an amplifying medium. The avoidance of self-focusing in these systems thus defines an important design criterion and makes the theoretical study of optical beam propagation in nonlinear media interesting not only from a fundamental point of view but from a practical engineering point of view as well.

In this article we describe a practical numerical scheme for solving the equations which describe the propagation of circularly symmetric beams in media whose dielectric properties can depend either linearly or nonlinearly on the electric field. Since the method is applicable to diffraction problems, the linear case can also be of considerable practical interest.

Certainly a variety of numerical difference schemes is available for this task. We have selected a technique which utilizes cubic splines, based upon the con-

* Work was performed under the auspices of the U.S. Atomic Energy Commission.

sideration that cubic splines lead to a solution having both continuous first and second derivatives and greater global accuracy over the entire interval between mesh points than do other schemes having a comparable order of accuracy. In any case, this article will serve as a model for the steps required in building a code for calculating self focusing in a cylindrical geometry.

1. Basic Differential Equations

For a circularly symmetric plane-polarized beam the electric field component satisfies the wave equation [1, 2]

$$\frac{1}{r}\left(\frac{\partial}{\partial r} r \frac{\partial E}{\partial r}\right) + \frac{\partial^2 E}{\partial z^2} - \frac{\epsilon_0}{c^2}\frac{\partial^2 E}{\partial t^2} - \frac{\epsilon_2}{c^2}\frac{\partial^2 (E)^2 E}{\partial t^2} = \frac{4\pi}{c^2}\frac{\partial^2 P}{\partial t^2}, \tag{1.1}$$

where cgs units have been used. In writing Eq. (1.1) it has been assumed that the dielectric permitivity ϵ can be expressed as the following nonlinear function of the field:

$$\epsilon = \epsilon_0 + \epsilon_2 E^2, \tag{1.2}$$

and that the effects of absorption or stimulated emission by the medium are contained in the polarization source term on the righthand side of Eq. (1.1). It is usual in treating Eq. (1.1) to make a slowly varying amplitude approximation in which E and P are expressed in the form

$$E = \mathscr{E}(r, z, t)\, e^{i(\omega t - kz)} + \text{c.c.}, \tag{1.3a}$$

$$P = p(r, z, t)\, e^{i(\omega t - kz)} + \text{c.c.}, \tag{1.3b}$$

where ω and k are respectively the frequency and wave number of the optical carrier wave, and where the slowly varying complex functions $\mathscr{E}$ and p satisfy

$$\begin{aligned} \frac{\partial^2 \mathscr{E}}{\partial z^2} &\ll k^2 \mathscr{E}, \\ \frac{\partial^2 \mathscr{E}}{\partial t^2} &\ll \omega^2 \mathscr{E}, \\ \frac{\partial^2 p}{\partial t^2} &\ll \omega^2 p. \end{aligned} \tag{1.4}$$

If expressions (1.3) are inserted into Eq. (1.1) and second derivatives are neglected in accordance with the inequalities (1.4), the following equation results:

$$\frac{\epsilon_0^{1/2}}{c}\frac{\partial \mathscr{E}}{\partial t} + \frac{\partial \mathscr{E}}{\partial z} + \frac{i}{2kr}\frac{\partial}{\partial r}\left(r\frac{\partial \mathscr{E}}{\partial r}\right) + \frac{3}{2}\frac{i\epsilon_2}{\epsilon_0} k \,|\, \mathscr{E} \,|^2 \mathscr{E} = -2\pi i \frac{\omega}{c\epsilon_0^{1/2}} p. \tag{1.5}$$

It is customary to replace the nonlinear expression (1.2) by a relation involving a nonlinear refractive index

$$n_r = n_0 + n_2\langle \mathscr{E}^2 \rangle, \tag{1.6}$$

where the bracket implies an average of the square of the field over a single optical cycle. The coefficient n_2 can be expressed in terms of ϵ_2 by

$$n_2 = \tfrac{3}{4}\epsilon_2/\epsilon_0^{1/2}. \tag{1.7}$$

It is also more convenient to normalize the field amplitude $\mathscr{E}$ to a variable $\mathscr{E}'$ such that $|\mathscr{E}'|^2$ is a measure of intensity. The magnitude S of the Poynting vector is given by

$$S = (c/4\pi)\langle EH \rangle = \epsilon_0^{1/2} c\,|\mathscr{E}|^2/2\pi. \tag{1.8}$$

Hence

$$\mathscr{E}' = (\epsilon_0^{1/2} c/2\pi)^{1/2}\,\mathscr{E}. \tag{1.9}$$

Defining further

$$\gamma = 4\pi n_2 k/\epsilon_0^{1/2} c \tag{1.10}$$

and

$$p' = i\,\frac{2\pi\omega}{c\epsilon_0^{1/2}}\left(\frac{\epsilon_0^{1/2} c}{2\pi}\right)^{1/2}, \tag{1.11}$$

we may then write Eq. (1.5) as

$$\frac{\epsilon_0^{1/2}}{c}\frac{\partial \mathscr{E}'}{\partial t} + \frac{\partial \mathscr{E}'}{\partial z} + \frac{i}{2kr}\frac{\partial}{\partial r}\left(r\frac{\partial \mathscr{E}'}{\partial r}\right) + i\gamma\,|\mathscr{E}'|^2\,\mathscr{E}' = -p\,. \tag{1.12}$$

In the simplest case p' describes the interaction between the electromagnetic field and a system of two level atoms. If the line broadening is homogeneous, i.e., if the resulting radiation has a Lorentz spectral shape, then p' is determined by the Bloch equations [6]

$$\partial p'/\partial t = T_2^{-1} p' = -(\sigma/2T_2)\, n\mathscr{E}', \tag{1.13a}$$

$$\hbar\omega\, \partial n/\partial t = 2p'\mathscr{E}'^{*} + \text{c.c.}, \tag{1.13b}$$

where n is the difference between the number density of atoms in the upper and lower states:

$$n = N_2 - N_1\,, \tag{1.13c}$$

σ is the radiation absorption cross section at line center, and T_2 is the atomic dipole dephasing time. The quantity T_2^{-1} is, of course, also equivalent to the half-width $\Delta\omega/2$ of the atomic line. If changes in p' are small during a time of the order of T_2, the solution of (1.12a) can be written approximately as

$$p' \cong -(\sigma/2)\, n\mathscr{E}', \tag{1.14}$$

and Eq. (1.12b) takes the familiar rate equation form

$$\hbar\omega\, \partial n/\partial t = 2\sigma n \mid \mathscr{E}' \mid^2. \tag{1.15}$$

Before proceeding with the analysis of Eq. (1.11) it is essential to introduce the transformation

$$\begin{aligned} t' &= t - (\epsilon_0^{1/2}/c)\, z, \\ z' &= z, \\ \mathscr{E}'(r, z, t) &= \mathscr{E}'(r, z', t') = \mathscr{E}'(r, z, t'). \end{aligned} \tag{1.16}$$

Equations (1.11) and (1.12) reduce to

$$\frac{\partial \mathscr{E}'}{\partial z'} + \frac{i}{2kr}\frac{\partial}{\partial r}\left(r\frac{\partial \mathscr{E}'}{\partial r}\right) + i\gamma \mid \mathscr{E}' \mid^2 \mathscr{E}' = -p', \tag{1.17a}$$

$$\frac{\partial p'}{\partial t'} + T_2^{-1} p' = -\frac{\sigma}{2T_2}\, n\mathscr{E}', \tag{1.17b}$$

$$\hbar\omega \frac{\partial n}{\partial t} = 2p'\mathscr{E}^*. \tag{1.17c}$$

In Eqs. (1.17) the 0 in the time variable t' refers to the actual time $t = (\epsilon_0^{1/2}/c) - z$ in a stationary frame, or the time of arrival of the front of the pulse at the position z. The system of Eqs. (1.17) is solved numerically by advancing all three dependent variables one step at a time along the z'-axis for each "time-slice" of the pulse, proceeding from the front of the pulse toward the back. The advantage of the coordinate transformation (1.16) is that it allows an accurate numerical scheme to be developed for which the increments in z' and t' need not be related in any special way, such as, for example, $\Delta z' = c\,\Delta t'/\epsilon_0^{1/2}$, which is required if Eq. (1.12) is integrated along characteristics. [6] Normally, the pulse is divided up into equal time intervals, and Δz is selected on the basis of changes in amplitude and phase from one axial step to the next. The solution of Eqs. (1.17b) and (1.17c) requires no special treatment beyond the requirements that these equations should be solved implicitly and self-consistently with Eq. (1.17a). (See for example Ref. [6].) No further discussion of the details of solving Eqs. (1.17b) and (1.17c)

will be given here, since our main concern will be Eq. (1.17a). It should be emphasized that the coupling between the radiation field and the material medium expressed in Eqs. (1.17b) and (1.17c) represents only one possibility of several. For example, the medium refractive index may be coupled to the medium density through hydrodynamic motion [4, 5], or it may be coupled to the electron number density if the medium is a plasma [7]. The nonlinear contribution to the refractive index may satisfy a relaxation equation if the medium is a molecular Kerr active liquid and the pulse of radiation is sufficiently short [8]. To emphasize the generality of the nonlinear contribution to the refractive index, we write Eq. (1.17a) in the form

$$i\frac{\partial \mathscr{E}}{\partial z} = \frac{1}{2kr}\frac{\partial}{\partial r}\left(r\frac{\partial \mathscr{E}}{\partial r}\right) + \chi\mathscr{E}, \tag{1.18}$$

where for convenience and simplicity the primes have been dropped from all variables, and the p' source term has been omitted. In other words, the most general time-dependent solution of Eq. (1.11) can be developed as a straightforward generalization of the solution of Eq. (1.18), which will now be the focus of our attention. Equation (1.18) is called the nonlinear wave equation in parabolic approximation and its equivalence in form to Schrödinger's time dependent wave equation should be obvious.

2. Requirements for a Practical Numerical Solution to the Parabolic Wave Equation

It goes without saying that in seeking a numerical solution to a given partial differential equation one demands an accurate as well as a flexible scheme. In the case of Eq. (1.18), accuracy requires among other things, that certain conservation conditions be met.

Writing Eq. (1.18) as

$$i\,\partial\mathscr{E}/\partial z = H\mathscr{E}, \tag{2.1}$$

where

$$H = \frac{i}{2kr}\frac{\partial}{\partial r}\left(r\frac{\partial}{\partial r}\right) + \chi, \tag{2.2}$$

and taking $z^{n+1} = z^n + \Delta z^n$, we may upgrade $\mathscr{E}$ in z by means of the Crank–Nicolson algorithm

$$\mathscr{E}^{n+1} = \frac{1 - i\Delta z^n \bar{H}/2}{1 + i\Delta z^n \bar{H}/2}\,\mathscr{E}^n, \tag{2.3}$$

which can be expressed in implicit form as

$$(1 + i\Delta z^n \bar{H}/2)\, \mathscr{E}^{n+1} = (1 - i\Delta z^n \bar{H}/2)\, \mathscr{E}^n. \tag{2.4}$$

Here $\bar{H}$ is gotten from H by substituting some average value $\bar{\chi}$ over the interval in question. If $\bar{H}$ is real, the operator on the right-hand side of Eq. (2.3) is Hermitian. The implicit scheme represented by Eq. (2.4) will, as a consequence, conserve energy and will be unconditionally stable. While the elements of $\bar{H}$ are real, only very special difference schemes can lead to forms of $\bar{H}$ which are symmetric. This latter requirement is necessary in order to guarantee that the eigen-values of $\bar{H}$ are real. In practice, however, any lack of symmetry in the operator $\bar{H}$ has proven to be unimportant, since implicit schemes of the form (2.4) always seem to conserve energy and guarantee unconditional stability. Explicit schemes have been widely used for solving Eq. (1.18) [9]. While such schemes have the advantage of being relatively easy to program, they are only conditionally stable and do not in general conserve beam energy. Thus the implicit scheme (2.4) is to be preferred both for reasons of accuracy and flexibility.

Conservation conditions also impose constraints on the radial discretization of Eq. (1.18). From (1.18) we find that conservation of total beam energy requires

$$\begin{aligned} i\frac{\partial}{\partial z}\int_0^{R_m} \mathscr{E}^* \mathscr{E} r\, dr &= \frac{1}{2k}\int_0^{R_m} \left[\mathscr{E}^* \frac{\partial}{\partial r}\left(r\frac{\partial \mathscr{E}}{\partial r}\right) - \mathscr{E}\frac{\partial}{\partial r}\left(r\frac{\partial \mathscr{E}^*}{\partial r}\right)\right] dr \\ &= \frac{1}{2k}\left[\mathscr{E}^* r\frac{\partial \mathscr{E}}{\partial r} - \mathscr{E} r\frac{\partial \mathscr{E}^*}{\partial r}\right]_0^{R_m} = 0, \end{aligned} \tag{2.5}$$

where R_m defines the extent of the region over which the numerical solution is to be determined. The rightmost expression in (2.5) can be made to vanish if either of the following boundary conditions is imposed at $r = R_m$

$$\mathscr{E}(R_m) = 0, \tag{2.6a}$$

$$(\partial \mathscr{E}/\partial r)|_{r=R_m} = 0. \tag{2.6b}$$

The avoidance of spurious boundary effects can be important if one is dealing with self-focusing. Experience has shown that the vanishing gradient condition tends to offer less of a boundary perturbation on the solution for a given R_m than does the vanishing field condition (2.6a). One may, however, safely use condition (2.6a) with a variable zone scheme if R_m can be made sufficiently large. For the remainder of the discussion we shall assume the condition (2.6b).

Let us assume now that the numerical solution is defined at radial points

$r = r_0, r_1, \ldots, r_j, \ldots, r = R_m$. Then Eq. (2.5) must be expressed in terms of sums of integrals taken over each cell j, or

$$i\frac{\partial}{\partial z}\sum_{j=1}^{j_m}\int_{r_{j-1}}^{r_j}\mathscr{E}^*\mathscr{E}r\,dr = \frac{1}{2k}\sum_{j=1}^{j_m}\int_{r_{j-1}}^{r_j}\left[\mathscr{E}^*\frac{\partial}{\partial r}\left(r\frac{\partial\mathscr{E}}{\partial r}\right) - \mathscr{E}\frac{\partial}{\partial r}\left(r\frac{\partial\mathscr{E}^*}{\partial r}\right)\right]dr$$

$$= \frac{1}{2k}\sum_{j=1}^{j_m}\left[\mathscr{E}^* r\frac{\partial\mathscr{E}}{\partial r} - \mathscr{E} r\frac{\partial\mathscr{E}^*}{\partial r}\right]_{r_{j-1}}^{r_j}$$

$$= \frac{i}{2k}\sum_{j=1}^{j_m} A^2\frac{\partial\phi}{\partial r}\Big|_{r_{j-1}}^{r_j} = 0, \tag{2.7}$$

where $\mathscr{E}$ has been expressed in terms of amplitude and phase as $\mathscr{E} = Ae^{i\phi}$.

For the right-hand side of (2.7) to vanish both $\mathscr{E}$ and $\partial\mathscr{E}/\partial r$ must be continuous at all points $r = r_j$ to insure continuity of the phase derivative

$$\partial\phi/\partial r = \text{Im}\,\mathscr{E}^{-1}\,d\mathscr{E}/dr,$$

and any numerical approximation of ϕ must reflect these continuity conditions, if energy is to be conserved. It is also desirable to maintain continuity of second derivatives as well in the numerical solution of Eq. (1.17). The quantity $d\phi/dr$ plays a central role in beam propagation, since it determines the direction and speed of energy flow. It is reasonable, therefore, to maintain the smoothness of this function and to avoid discontinuities in its first derivative in setting up a numerical scheme. However, it is simpler to base a numerical scheme for Eq. (1.17) on a complex field amplitude that is expressed in terms of its real and imaginary parts, rather than in terms of amplitude and phase variables. If it is desired to monitor the phase and the phase gradient as the calculation proceeds for diagnostic purposes or to gain insight into the behavior of calculated intensity patterns, it will be necessary to calculate these quantities numerically from the solution for $\mathscr{E}$. In order to do this an accurate knowledge of ϕ and its derivatives at the points of the mesh is required.

A final requirement on the numerical solution method is that it should allow the propagating field to be always accurately defined on the given mesh. This may pose a problem if the beam energy is caused to either strongly converge or diverge due to intensity induced changes in the refractive index. Strong self-focusing in the neighborhood of intensity maxima is an example of this. If one knows in advance how the beam will focus or spread it should be possible to introduce finer zoning in regions where it is required. Thus accuracy and flexibility require the capability of introducing a variable mesh spacing. An additional advantage of variable mesh spacing is that it enables boundary effects to be reduced to a minimum through the use of large zone sizes near the mesh boundary.

Thus, the various requirements of continuity, flexibility, and accuracy listed

above suggest the use of a cubic spline applicable to a grid with variable spacing. The Laplacian

$$\frac{1}{r}\frac{\partial}{\partial r}\left(r\frac{\partial \mathscr{E}}{\partial r}\right) = \frac{\partial^2 \mathscr{E}}{\partial r^2} + \frac{1}{r}\frac{\partial \mathscr{E}}{\partial r}, \tag{2.8}$$

however, contains a singularity at the origin due to the term proportional to $1/r$. It is therefore convenient to construct a spline which is based on a piecewise linear Laplacian rather than a second derivative in r which is piecewise linear. If the Laplacian is continuous, the second derivative of $\mathscr{E}$ will, of course, also be continuous. We shall henceforth refer to these splines as cylindrical cubic splines.

3. Derivation of Cylindrical Cubic Spline Equations

If the Laplacian is to be continuous and piecewise linear [10], it must satisfy

$$\frac{1}{r}\frac{\partial}{\partial r}\left(r\frac{\partial \mathscr{E}}{\partial r}\right) = \frac{M_{j-1}}{l_j}(r_j - r) + \frac{M_j}{l_j}(r - r_{j-1}) \tag{3.1}$$

for $r_{j-1} < r < r_j$ and $j = 1, 2, \ldots, j_m$, where

$$l_j = r_j - r_{j-1}. \tag{3.2}$$

Integrating Eq. (3.1) once gives

$$\frac{\partial \mathscr{E}}{\partial r} = \frac{M_{j-1}}{l_j} r\left(\frac{r_j}{2} - \frac{r}{3}\right) + \frac{M_j}{l_j} r\left(\frac{r}{3} - \frac{r_{j-1}}{2}\right) + \frac{C_j}{r}, \tag{3.3}$$

and integrating Eq. (3.3) yields

$$\mathscr{E} = \frac{M_{j-1}}{l_j} r^2\left(\frac{r_j}{4} - \frac{r}{9}\right) + \frac{M_j}{l_j} r^2\left(\frac{r}{9} - \frac{r_{j-1}}{4}\right) + C_j \ln r + D_j. \tag{3.4}$$

Finiteness at the origin requires that

$$C_1 = 0, \qquad D_1 = \mathscr{E}_0. \tag{3.5}$$

The constants C_j and D_j for the remaining intervals are determined by the requirement that

$$\mathscr{E}(r_j) = \mathscr{E}_j, \qquad j = 0, 1, 2, \ldots, j_m. \tag{3.6}$$

Applying condition (3.6) to Eq. (3.4) at $r = r_j$ and $r = r_{j-1}$ yields, after a little algebra,

$$\begin{aligned}\mathscr{E} = &\frac{M_{j-1}}{l_j} r^2 \left(\frac{r_j}{4} - \frac{r}{9}\right) + \frac{M_j}{l_j} r^2 \left(\frac{r}{9} - \frac{r_{j-1}}{4}\right) \\ &+ [\alpha_j M_j + \beta_j M_j + \gamma_j(\mathscr{E}_j - \mathscr{E}_{j-1})] \ln r \\ &+ \alpha_j' M_j + \beta_j' M_{j-1} + \gamma_{1j}' \mathscr{E}_j - \gamma_{2j}' \mathscr{E}_{j-1}, \end{aligned} \tag{3.7}$$

where α_j, β_j, γ_j, α_j', β_j', γ_{1j}', and γ_{2j}' are defined by

$$\alpha_j = \left[r_j^2 \left(\frac{r_{j-1}}{4} - \frac{r_j}{9}\right) - r_{j-1}^2 \left(\frac{r_{j-1}}{4} - \frac{r_{j-1}}{9}\right)\right] \Big/ l_j \left[\ln \left(\frac{r_j}{r_{j-1}}\right)\right], \tag{3.8a}$$

$$\beta_j = \left[r_j^2 \left(\frac{r_j}{9} - \frac{r_j}{4}\right) - r_{j-1}^2 \left(\frac{r_{j-1}}{9} - \frac{r_j}{4}\right)\right] \Big/ l_j \left[\ln \left(\frac{r_j}{r_{j-1}}\right)\right], \tag{3.8b}$$

$$\gamma_j = 1 \Big/ \left[\ln \left(\frac{r_j}{r_{j-1}}\right)\right], \tag{3.8c}$$

$$\gamma_{1j}' = \ln r_{j-1} \Big/ \ln \left(\frac{r_{j-1}}{r_j}\right), \tag{3.8d}$$

$$\gamma_{2j}' = \ln r_j \Big/ \ln \left(\frac{r_{j-1}}{r_j}\right), \tag{3.8e}$$

$$\alpha_j' = \left[(\ln r_{j-1})\, r_j^2 \left(\frac{r_{j-1}}{4} - \frac{r_j}{9}\right) - \ln(r_j)\, r_{j-1}^2 \left(\frac{r_{j-1}}{4} - \frac{r_{j-1}}{9}\right)\right] \Big/ l_j \ln \left(\frac{r_{j-1}}{r_j}\right), \tag{3.8f}$$

$$\beta_j' = \left[\ln(r_{j-1})\, r_j^2 \left(\frac{r_j}{9} - \frac{r_j}{4}\right) - (\ln r_j)\, r_{j-1}^2 \left(\frac{r_{j-1}}{9} - \frac{r_j}{4}\right)\right] \Big/ l_j \ln \left(\frac{r_{j-1}}{r_j}\right). \tag{3.8g}$$

Equations (3.8) are valid for $j = 1, 2, \ldots, j_m$. For $j = 1$ we have, on account of (3.5)

$$\alpha_1 = \beta_1 = \gamma_1 = 0, \tag{3.9a}$$

$$\alpha_{11}' = \beta_{11}' = \gamma_{11}' = 0, \tag{3.9b}$$

$$\gamma_{21}' = -1. \tag{3.9c}$$

Differentiating Eq. (3.7) yields

$$\begin{aligned}\frac{\partial \mathscr{E}}{\partial r} = &M_j \left[\frac{\alpha_j}{r} + \frac{r}{l_j}\left(\frac{r}{3} - \frac{r_{j-1}}{2}\right)\right] + M_{j-1}\left[\frac{\beta_j}{r} + \frac{r}{l_j}\left(\frac{r_j}{2} - \frac{r}{3}\right)\right] \\ &+ \frac{\gamma_j}{r}(\mathscr{E}_j - \mathscr{E}_{j-1}). \end{aligned} \tag{3.10}$$

If we demand continuity of $\partial \mathscr{E}/\partial r$ at $r = r_j$, then the M_j must satisfy

$$A_j M_{j+1} + B_j M_j + C_j M_{j-1} = -\frac{\gamma_{j+1}}{r_j}(\mathscr{E}_{j+1} - \mathscr{E}_j) + \frac{\gamma_j}{r_j}(\mathscr{E}_j - \mathscr{E}_{j-1}), \quad (3.11)$$

where A_j, B_j, and C_j are defined by

$$A_j = \frac{\alpha_{j+1}}{r_j} + \frac{r_j}{l_{j+1}}\left(\frac{r_j}{3} - \frac{r_j}{2}\right), \quad (3.12a)$$

$$B_j = \frac{\beta_{j+1}}{r_j} + \frac{r_j}{l_{j+1}}\left(\frac{r_{j+1}}{2} - \frac{r_j}{3}\right) - \frac{\alpha_j}{r_j} - \frac{r_j}{l_j}\left(\frac{r_j}{3} - \frac{r_{j-1}}{2}\right), \quad (3.12b)$$

$$C_j = -\frac{\beta_j}{r_j} - \frac{r_j}{l_j}\left(\frac{r_j}{2} - \frac{r_j}{3}\right). \quad (3.12c)$$

Equation (3.11) enables the M_j to be determined in terms of the $\mathscr{E}_j$ values by the simple back substitution algorithm for inverting a tri-diagonal matrix [11]. When the M_j are known, Eq. (3.7) in conjunction with Eqs. (3.8) can be used to construct the function $\mathscr{E}(r)$ with continuous first and second derivatives over the entire interval $0 \leqslant r \leqslant r_{j_m}$. Conversely, the differential Eq. (1.17) after it has been differenced with respect to z can be used to eliminate M_j in terms of $\mathscr{E}_j$. If the resulting expression is then substituted into Eq. (3.11), a difference equation in $\mathscr{E}_j$ in tri-diagonal form results. The solution to the difference equation represents a numerical approximation to Eq. (1.17) with continuous first and second derivatives.

One may also develop a similar scheme for solving the diffusion equation

$$\frac{\partial \psi}{\partial t} = \frac{1}{r}\frac{\partial}{\partial r}\left(rD\frac{\partial \psi}{\partial r}\right), \quad (3.13)$$

where ψ represents a density variable, but in this case one must require continuity of the "leakage" rate L and the current J, where

$$L = \frac{1}{r}\frac{\partial}{\partial r}\left(rD\frac{\partial \psi}{\partial r}\right), \quad (3.14a)$$

$$J = D\frac{\partial \psi}{\partial r}. \quad (3.14b)$$

The analysis follows as before, and one obtains in place of Eq. (3.11) the following relation for a stepwise constant diffusion coefficient

$$A_j L_{j+1} + B_j L_j + C_j L_{j-1} = -\frac{D_{j+1/2}\gamma_{j+1}}{r_j}(\psi_{j+1} - \psi_j) + \frac{D_{j-1/2}\gamma_j}{r_j}(\psi_j - \psi_{j-1}), \quad (3.15)$$

where $D_{j-1/2}$ and $D_{j+1/2}$ are the values of D centered within the intervals $r_{j-1} < r < r_j$ and $r_j < r < r_{j+1}$, respectively.

4. Derivation of Difference Form for Wave-Equation

Let us write Eq. (1.17) in the form

$$i\,\partial\mathscr{E}/\partial z = (1/2k)\,M + \bar{\chi}\mathscr{E}. \tag{4.1}$$

For the nonlinear function $\bar{\chi}$ one may take its value at the previous z-step or a suitable prediction of its value at $z = z_m{}^n + \Delta z/2$. If Eq. (4.1) is now integrated from $z_m{}^n$ to z^{n+1} at $r = r_k$, the result is

$$\mathscr{E}_j^{n+1} - \mathscr{E}_j{}^n = -(i\Delta z/4k)(M_j^{n+1} + M_j{}^n) - (i\Delta z/2)\,\bar{\chi}_j(\mathscr{E}_j^{n+1} + \mathscr{E}_j{}^n). \tag{4.2}$$

Or, solving from M_j^{n+1},

$$M_j^{n+1} = X_j\mathscr{E}_j^{n+1} + Y_j\,, \tag{4.3}$$

where

$$X_j = 2k[(2i/\Delta z) - \bar{\chi}_j], \tag{4.4a}$$

$$Y_j = -2k[(2i/\Delta z) + \bar{\chi}_j]\,\mathscr{E}_j{}^n - M_j{}^n. \tag{4.4b}$$

We now substitute expression (4.3) into Eq. (3.11) obtaining

$$\mathscr{E}_{j+1}^{n+1}[A_jX_{j+1} + (\gamma_{j+1}/r_j)] + \mathscr{E}_j^{n+1}[B_jX_j - (\gamma_{j+1} + \gamma_j)/r_j] + \mathscr{E}_{j-1}^{n+1}[C_jX_{j-1} + (\gamma_j/r_j)]$$
$$= -[A_jY_{j+1} + B_jY_j + C_jY_{j-1}]. \tag{4.5}$$

Equation (4.5), which has tri-diagonal form, represents the final difference equation which $\mathscr{E}_j^{n+1}$ must satisfy at all interior points and must be solved in conjunction with boundary conditions at $r = 0$ and $r = r_{j_m}$. Note that the M^n may be eliminated from Eqs. (4.4b) and (4.5) through the use of Eq. (3.11), and a saving in storage made if desired.

We will require that $\partial E/\partial r$ vanish at $r = 0$ and $r = r_{j_m}$, which requires setting expression (3.10) equal to 0 at those points. Due to the presence of the spline coefficients M_j and M_{j-1} in Eq. (3.10), two more arbitrary conditions are required

to eliminate the boundary values of these quantities. There are three obvious possibilities, namely,

$$M_{j_m} = M_{j_{m-1}}, \tag{4.6a}$$

$$M_0 = M_1; \qquad \text{quadratic condition},$$

$$M_{j_m} = M_0 = 0; \qquad \text{flex condition}, \tag{4.6b}$$

$$M_0^{n+1} = X_0 \mathscr{E}_0^{n+1} + Y_0, \tag{4.6c}$$

$$M_{j_m}^{n+1} = X_{j_m} \mathscr{E}_{j_m}^{n+1} + Y_{j_m}; \qquad \text{differential equation condition}.$$

Condition (4.6c) is equivalent to requiring that the differential equation be satisfied at the boundary points. All three of these conditions have been tried, and they all give satisfactory results. However, the application of condition (4.6c) *at the origin* gives the best results for situations involving focusing along the z-axis. Therefore it is the preferred condition at the origin.

5. Calculation of Phases, Axial Space Increments, and Related Matters

A determination of the phase of $\mathscr{E}$ can be made in terms of a numerical evaluation of the logarithmic derivative of $\mathscr{E}$:

$$\frac{d\phi}{dr}\bigg|_{r=r_j} = \operatorname{Im}\left(\frac{1}{\mathscr{E}}\frac{\partial \mathscr{E}}{\partial r}\right)_{r=r_j}. \tag{5.1}$$

The derivative $\partial \mathscr{E}/\partial r$ is evaluated using expression (3.10), and the phase is then calculated by numerically evaluating the integral

$$\phi(r_j) = \int_0^{r_j} \left(\frac{d\phi}{dr}\right) dr. \tag{5.2}$$

Equation (5.2) assigns the value 0 to the phase at the origin. For evaluating the integral the trapezoidal rule is sufficiently accurate.

One maximizes both calculation efficiency and accuracy by selecting a new value for the axial space increment Δz for each integration cycle, based on the rate of change of both the amplitude and phase of the field. Writing

$$\mathscr{E} = Ae^{i\phi}, \tag{5.3}$$

one may obtain an expression for the relative change in A and the absolute change in ϕ by taking

$$\delta A_j/A_j = \mathrm{Re}[(\mathscr{E}_j^{n+1} - \mathscr{E}_j^{n})/\mathscr{E}_j^{n+1}], \tag{5.3a}$$

$$\delta\phi_j = \mathrm{Im}[(\mathscr{E}_j^{n+1} - \mathscr{E}_j^{n})/\mathscr{E}_j^{n+1}]. \tag{5.3b}$$

The value of Δz to be used in the next integration cycle, Δz^{n+1}, is obtained from the value Δz^n used in the cycle just completed by means of the relation

$$\Delta z^{n+1}/\Delta z^n = R/\mathrm{Max}(|\,\delta A/A\,|, |\,\delta\phi\,|), \tag{5.4}$$

where the Max function is equal to the maximum of its arguments, and where the arguments are computed using Eqs. (5.3a) and (5.3b). The input number R represents the largest fractional amplitude or absolute phase change which will be tolerated.

Caution should be used in applying condition (5.4) over the entire domain of integration, i.e., over all points r_j, or else the step size may be controlled by boundary effects or erratic variations in the field in regions where the amplitude is relatively small and unimportant. Consequently, one should select a region where the Δz test is to be applied. In addition, one may wish to apply criterion (5.4) only if the local amplitude is greater than some prescribed value.

6. Numerical Examples

Figure 1 shows the evolution of a Fresnel diffraction pattern which leads to self-focusing [12]. The initial radial intensity distribution of the beam is Gaussian shaped before it is passed through an aperture located at a radius of .5 cm. The initial intensity pattern at $z = 0$ is shown in the bottom left hand corner of Fig. 1 for the maximum intensity in the pulse. Note that the intensity is allowed to fall to 0 exponentially rather than by experiencing a sudden drop. Some form of pulse shape tailoring at the aperture boundary is essential since the spline basis functions are not suited to discontinuous behavior. An exponential is neither unique nor is it the best choice either, although it certainly leads to acceptable results. Care must be used in tailoring the intensity distribution beyond the aperture radius to avoid undue influence on the diffraction pattern. The propagation path consists of three air layers alternating with neodymium doped glass rod amplifiers 23 cm in length. Starting with the plot for $z = 108$ cm, which represents the intensity distribution at the entrance to the first rod the plots alternately represent intensity distributions at the rod input and output faces. Self-focusing is well advanced at 207 cm, which is 15 cm into the final rod, in agreement with experimental

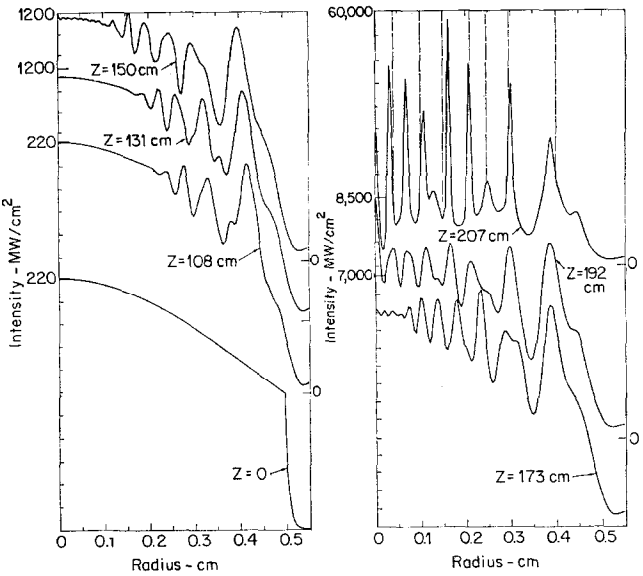

FIG. 1. Evolution of Fresnel and self-focusing pattern for laser amplifier system consisting of rods and air gaps. Aperture is placed at $z = 0$, truncating Gaussian shaped beam. Beginning with $z = 108$ cm, each pair of curves indicates intensity distributions at the entrance and exit faces of a rod amplifier. Graph for $z = 207$ cm indicates self-focusing in final rod where damage was experimentally observed. Central maximum is off scale. Dotted vertical lines in pattern for $z = 207$ cm indicate position of fringes actually observed in damage pattern [12].

observations of damage to the glass rod. The damage takes the form of a Fresnel ring pattern at the output face of the final rod. Dotted lines in Fig. 1 indicate the position of the experimentally observed rings. The calculation was carried out with 120 equally spaced zones within the illuminated area of the aperture, i.e., between $r = 0$ and $r = .5$ cm; 30 zones increasing in size completed the domain of integration which extended to $r = 1.0$ cm. The problem was run with a constant Δz-step in the air that corresponded to the condition $\Delta z = 2k(\Delta r)^2$, where Δr is the constant zone size referred to above.

Figures 2 and 3 show the results of focusing a beam having a Gaussian intensity profile with a 15 cm focal length lens. The initial field amplitude is given by

$$\mathscr{E}(r, 0) = \mathscr{E}_0 \exp[-r^2/2\sigma^2 + ikr^2/2z_f], \tag{5.11}$$

where σ is the $1/e$ intensity radius. The parabolic phase front causes the beam to focus at a position $z = z_f$. The solution to Eq. (1.18) with $\bar{\chi} = 0$ and (5.11) as an initial condition can be represented analytically [13] and results in an amplitude distribution which always remains Gaussian. However, this problem

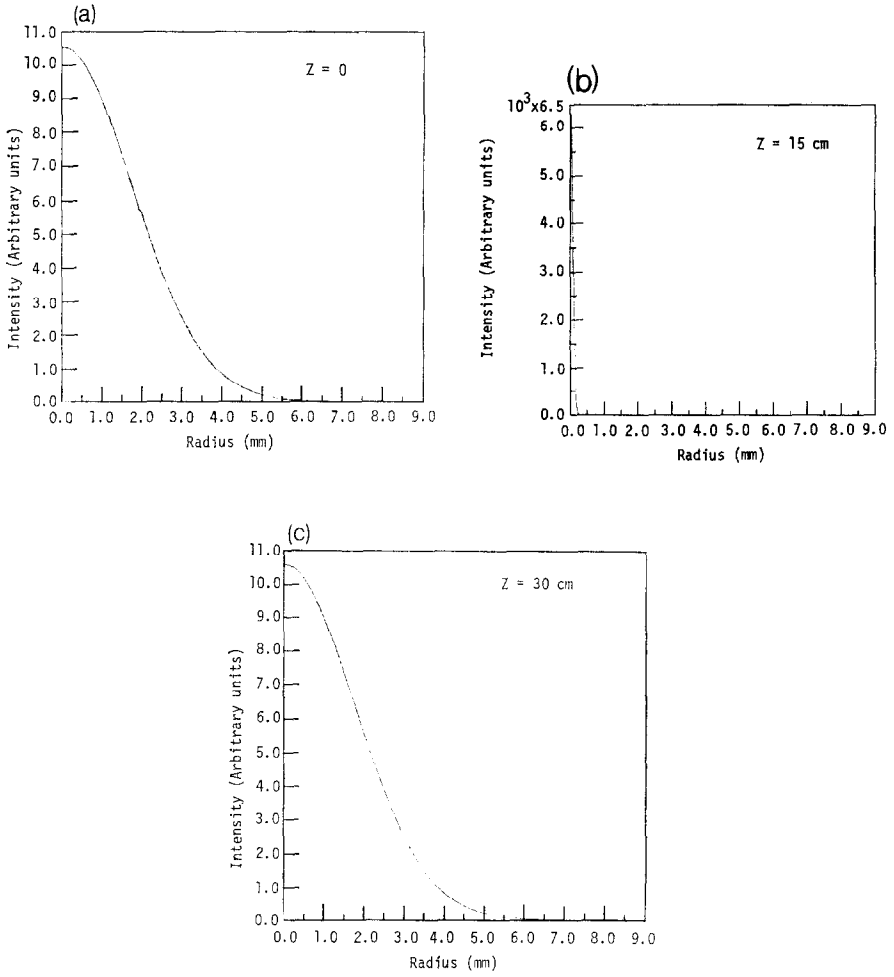

FIG. 2. Calculated intensity distributions as functions of radius for Gaussian shaped beam. Initial $1/e$ intensity radius is 0.25 cm, wavelength is 10.6 μm, and focal length of lens is 15 cm. (a) Initial intensity distribution. (b) Intensity distribution in focal plane. Only 14 points represent field within $1/e$ intensity radius. (c) Intensity distribution at one focal length beyond focal plane.

is an excellent test of the numerical method, since any disturbance of the phase front will make it impossible to carry the solution through the focal plane at $z = z_f$. In particular, phase variations with z are rapid in the neighborhood of the focal plane, requiring suitably small values of Δz if the wave is to remain intact after passing through the focus. The use of an adaptive integration step as prescribed by Eq. (5.4) clearly removes any difficulty in advancing the solution

in the focal region. The solution depicted in Figs. 2 and 3 was obtained using 1000 equally spaced radial points and allowing a 0.05 fractional change in amplitude and the same absolute change in phase per cycle [14]. The initial $1/e$ intensity radius was 0.25 cm and the wavelength was 1.06×10^{-3} cm. The initial value of Δz was taken to be 0.2 cm. The self-adjusted value of Δz near the focus was .02 cm. The number of cycles required to integrate to a distance $z = 2z_f = 30$ cm

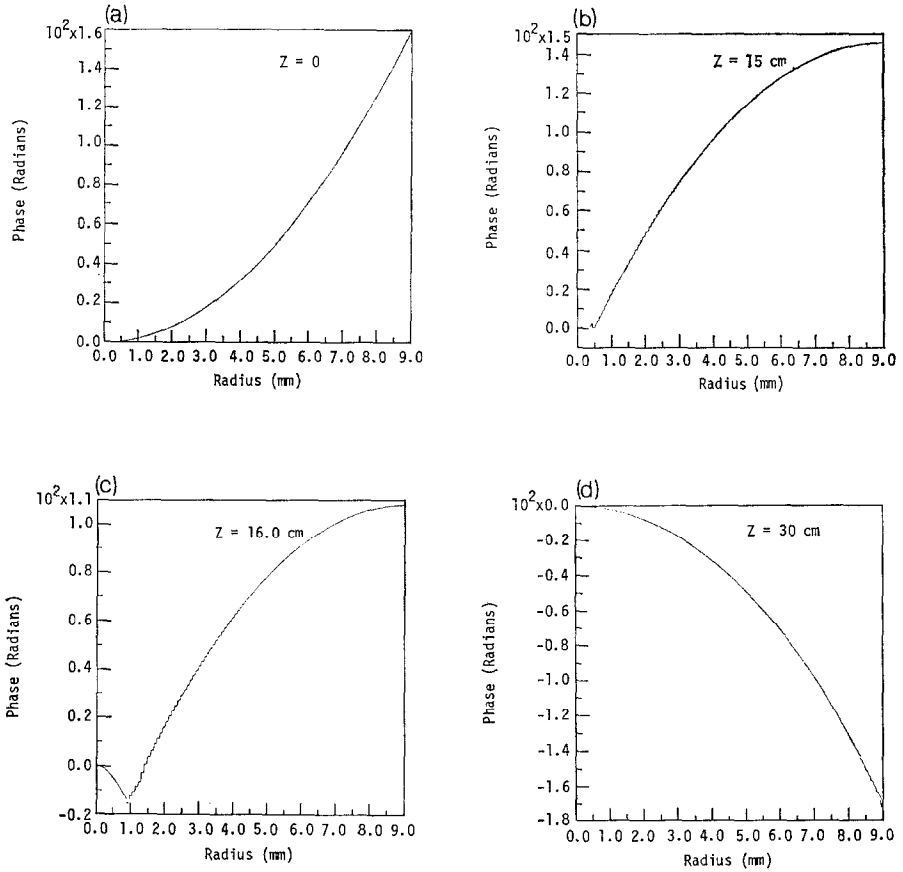

FIG. 3. Phase distributions as functions of radius for focused Gaussian beam described in Fig. 2. (a) Initial phase at $z = 0$. (b) Phase in focal plane, indicating stationarity over portion of beam where most of energy is located. (c) Phase 1 cm beyond focal plane. Curvature has reversed indicating a diverging beam. (d) Phase at one focal length beyond focal plane. Phase distribution is negative of phase distribution for $z = 0$, except for minor diffractive changes and boundary effect.

was 1221. Figure 1 shows the intensity distribution at $z = 0$, $z = z_f$, and $z = 2z_f$. At the focus the intensity distribution is represented by only 14 points within the $1/e$ radius of the Gaussian. However, this does not prevent the correct Gaussian shape from emerging at $z = 2z_f$. It will be noted that at $z = 0$ the on-axis intensity is 1.06 whereas at $z = 2z_f$ it is 1.05. This slight drop in peak intensity is due to a small amount of diffractive spreading of the wave. The initial phase as a function of radius is shown in Fig. 3a. Phase distributions at $z = z_f = 15$ cm, $z = 16$ cm, and $z = 2z_f = 30$ cm are shown in Figs. 3b, 3c, and 3d. The phase should be stationary, i.e., $d\phi/dr = 0$, at $z = z_f$. This is true over the portion of the beam containing nearly all of the energy. Figure 3c shows the phase at a position just 1 cm beyond the focal plane. Note that the curvature of the phase has reversed, as it should, since the beam is now diverging. The behavior of the phase is correct in the portion of the beam containing most of the energy. Figure 3d shows the phase distribution at $z = 2z_f = 30$ cm. It is clearly the negative of the one for $z = 0$. A very slight perturbation in the phase is seen to occur near the boundary, which is due to the imposition of a boundary condition. In the present example the flex condition (4.6b) was employed. The calculated beam energy at the finish of the problem differed from the input energy only in the fifth significant figure. The difference is probably more of an indication of the accuracy of the trapezoidal integration employed in determining the energy than it is a reflection of non-conservation of energy.

REFERENCES

1. R. Y. CHIAO, E. GARMIRE, AND C. H. TOWNES, *Phys. Rev. Lett.* **13** (1964), 479.
2. P. L. KELLEY, *Phys. Rev. Lett.* **15** (1965), 1005.
3. S. A. AKHMANOV, A. P. SUKHORUKOV, AND R. V. KHOKHLOW, *Usp. Fiz. Nauk* **93** (1967), 19 [*Sov. Phys.—Usp.* **93** (1968), 609].
4. J. WALLACE AND C. M. CAMAC, *J. Opt. Soc. Am.* **60** (1970), 1587.
5. A. H. AITKEN, J. N. HAYES, AND P. B. ULRICH, Propagation of high-energy 10.6 micron laser beams through the atmosphere, Report NRL-7293, Naval Research Laboratory, Washington, DC, 1971; J. HERRMANN AND L. C. BRADLEY, Numerical calculation of light propagation, Report LTP-10, M.I.T. Lincoln Laboratory, Lexington, MA, 1971.
6. J. A. FLECK, JR., *Phys. Rev. B* **1** (1970), 84.
7. M. D. FEIT AND J. A. FLECK, JR., *Appl. Phys. Lett.* **24** (1974), 169.
8. J. A. FLECK, JR., AND P. L. KELLEY, *Appl. Phys. Lett.* **15** (1969), 313; J. A. FLECK, JR., AND R. L. CARMAN, *Appl. Phys. Lett.* **20** (1972), 290; F. SHIMIZU, *IBM J. Res. Develop.* **17** (1973), 286.
9. See for example, H. F. HARMUTH, *J. Math. Phys.* **36** (1957), 269.
10. For a discussion of ordinary cubic splines see, for example, J. L. WALSH, J. H. AHLBERG, AND E. N. NELSON, *J. Math. Mech.* **11** (1962), 225.
11. ROBERT D. RICHTMYER AND K. W. MORTON, "Difference Methods for Initial-Value Problem," pp. 198–201, Interscience, New York, 1967.

12. J. A. FLECK, JR., AND C. LAYNE, *Appl. Phys. Lett.* **22** (1973), 467.
13. See for example, H. KOGELNIK AND T. LI, *Appl. Opt.* **5** (1966), 1550.
14. The size of the allowable fractional change in amplitude and change in phase per cycle vary from problem to problem. In the present problem of linear focusing a value of 0.05 is adequate, whereas in a problem involving self-focusing a value of 0.01 may be required.